Substrate-Wrapped, Single-Walled Carbon Nanotube Probes for Hydrolytic Enzyme Characterization

Nathaniel E. Kallmyer, Joseph Musielwicz, Joel Sutter, and Nigel Forest Reuel

Anal. Chem., **Just Accepted Manuscript** • DOI: 10.1021/acs.analchem.7b05444 • Publication Date (Web): 20 Mar 2018

Substrate-Wrapped, Single-Walled Carbon Nanotube Probes for Hydrolytic Enzyme Characterization

*Nathaniel E. Kallmyer, Joseph Musielewicz, Joel Sutter, Nigel F. Reuel**

*Corresponding Author: Prof. Nigel F Reuel
Iowa State University, 2114 Sweeney Hall
618 Bissell Rd. Ames, IA
50011, United States
reuel@iastate.edu
Ph: 515-294-4592

Abstract

Hydrolytic enzymes are a topic of continual study and improvement due to their industrial impact and biological implications; however, the ability to measure the activity of these enzymes, especially in high-throughput assays, is limited to an established, few enzymes and often involves the measurement of secondary byproducts or the design of a complex degradation probe. Herein, a versatile single-walled carbon nanotube (SWNT)-based biosensor that is straightforward to produce and measure is described. The hydrolytic enzyme substrate is rendered as an amphiphilic polymer which is then used to solubilize the hydrophobic nanotubes. When the target enzyme degrades the wrapping, SWNT fluorescent signal is quenched due to increased solvent accessibility and aggregation, allowing quantitative measurement of hydrolytic enzyme activity. Using (6,5) chiral SWNT suspended with polypeptides and polysaccharides, turnover frequencies are estimated for cellulase, pectinase, and bacterial protease. Responses are recorded for concentrations as low as 5 fM using a well-characterized protease, Proteinase K. An established trypsin-based plate reader assay is used to compare this nanotube probe assay with standard techniques. Furthermore, the effect of freeze-thaw cycles and elevated temperature on enzyme activity is measured, suggesting freezing to have minimal impact even after 10 cycles and heating to be detrimental above 60°C. Finally, rapid optimization of enzyme operating conditions is demonstrated by generating a response surface of cellulase activity with respect to temperature and pH to determine optimal conditions within 2 hours of serial scans.

Keywords: Enzyme assay, Single-Walled Carbon Nanotubes, Biosensor, Quench

1. Introduction

Hydrolytic enzymes play critical roles in natural biological systems and have emerged as significant designed products for modern biotechnological processes. These enzymes are classified together (Enzyme Class 3) based on their ability to catalyze the hydrolysis of chemical bonds; sub-classifications reveal the breadth of activities these enzymes have developed, cleaving the following bonds: esters (EC 3.1), glycosylic (EC 3.2), ether (EC 3.3), peptides (EC 3.4), C-N other than peptides (EC 3.5), acid anhydrides (EC 3.6), C-C (EC 3.7), halide (EC 3.8), P-N (EC 3.9), S-N (EC 3.10), C-P (EC 3.11), S-S (EC 3.12), and C-S (EC 3.13)[1]. In nature, these enzymes are the recyclers of bulk materials, breaking down proteins, carbohydrates, and fats into their constitutive parts to make available smaller building blocks for new biological assembly. Hydrolytic enzymes also have natural, prominent roles in disease[2]. For plants, pathogenic bacteria and pests can excrete enzymes to breakdown the recalcitrant cell walls to help their invasion[3,4]. In cancer, tumors secrete a class of matrix metalloproteinases (MMP) that are responsible for reconfiguring healthy tissue into a permeable matrix that allows for tumor growth and metastasis[5]. Engineered product examples of hydrolytic enzymes include the use of hydrolases in detergent to aid in stain removal, animal feed to aid in digestion, paper pulp preparation, and food processing such as cheese making, leather tanning, biofuels, juice clarification, baking, brewing, sugaring, and meat processing[6]. For these engineered enzyme applications, an entire industry has grown around the optimization and design of more stable and efficient enzymes for process use, with an overall industrial enzyme market size of $4.2 billion in 2014 and predicted growth to $6.2 billion in 2020 with hydrolytic enzymes accounting for 75% of these products[7,8].

Although our understanding of hydrolytic enzyme function and design has improved in the last century, one significant limiting factor in our study and design of these catalysts is the ability to measure their activity and selectivity in real time with a modular tool. Specialized probes and techniques have been developed to screen hydrolytic activity, including FRET-based probes, chromogenic substrate analogs, indirect measurement of substrate by correlations, and single-point colorimetric assays (Table 1).

Table 1: Methods of Detecting Hydrolytic Activity

Method	Transducer	Strengths	Limitations
FRET and BRET-based probes	Organic dyes[9]	Established linking chemistry protocols, Discrete fluorescent peaks[10]	Photobleaching, Some toxic dyes[10]
	Quantum dots[11]	High quantum yield in near-infrared window[10], High reliability and sensitivity[12]	"Blinking," Few linking chemistry protocols available, Large molecular size[10], Cytotoxicity[13], Low FRET Efficiency[14]
	Luciferase[15]	Stability in biological media, High sensitivity[16]	Must be paired with fluorophore, Requires luciferase substrate
Substrate structural analogs	Organic chromogenic substrates[17]	Easily implemented, minimal preparation	Relatively low sensitivity[18]
Indirect measurement of substrate	Viscosimetry[19]	Directly applicable to multiple polymers[20]	Nonlinear response[21], Sensitive to matrix elements
	Turbidimetry[22]	Functional for	Other causes of turbidity,

		immiscible or insoluble reagents or products	Nonlinear short-term response[23], Single-point nephelometric measurements[24]
Single-point assays	Colorimetric or amperometric product assay[25,26]	Well-established[25]	Time-intensive colorimetric assays, Variable linear dynamic range, Susceptible to interference[27,28]

To overcome the limitations of other optical sensors, namely the signal quality and synthesis complexity, single-walled carbon nanotubes (SWNT) may be used as a fluorescent transducer, offering high assay sensitivity and the advantage of a near-infrared emission window which more effectively penetrates complex samples[29].

Semi-conducting SWNT are an established platform for biological sensing. They are naturally fluorescent due to their unique 1-D, energy of states distribution[30]. The fluorescence of the nanotube is sensitive to changes in the SWNT surface dielectric environment[31]. This sensitivity has been exploited to design sensors for small molecules[32–34], sugars[35,36], metabolites[37], DNA[38], proteins[39], and glycans[40]. Furthermore, the near-infrared fluorescence of SWNT are very photostable with demonstrated *in vivo* detection on month-to-year timeframes[41,42]. The quantitative detail of these sensors can map large ensemble kinetic distributions all the way down to single molecule binding kinetics[40,43]. Some of these sensors include tethered selection agents, such as capture proteins[39], to selectively bind the desired analyte; more recent advances simply exploit the wrapped polymer which forms a nanotube 'corona' with specific conformation on the nanotube forming selective pockets and patches to which the analyte binds[44,45]. The innovation of the sensor presented here is an astute inversion of these recent works, to exploit the surface sensitivity by intentional *degradation* of the nanotube 'corona' rather than binding.

2. Experimental Section

2.1. Sensor Synthesis

To prepare wrapped nanotube solutions, 2.5 mg SWNT (Sigma, 704148) were sonicated in 5 mL substrate solution using a probe sonicator (Qsonica CL-18) for 30 minutes at 15 W. The mixture was then sonicated twice for 15 minutes at 9000 xg. SWNT were sonicated in 10 mg/mL pectin, casein, and carboxymethylcellulose (CMC) solutions and 2.5 mg/mL bovine serum albumin (BSA) and lysozyme solutions. The sensors were recovered in the supernatant. Substrate concentrations were selected based on solubility and presumed affinity to SWNT.

2.2. Fluorescent Assay

BSA (Carolina 842251)-wrapped SWNT were tested with Alcalase bacterial protease pellets (Carolina 202390). Citrus pectin (Sigma P9135)-wrapped SWNT were tested with Pectinex pectinase (Carolina, 202380). CMC (Sigma 419303)-wrapped SWNT were tested with a cellulase mix (Carolina 853630). Samples were tested serially in a 96-well plate with 3-5 minute scan times. Enzyme samples were added approximately 30 s into each scan to establish an initial baseline.

2.3. Establishing Detection Limit

BSA-wrapped SWNT were tested with a Proteinase K (NEB P8107S) sample that was serially diluted from 20 mg/mL to 2 pg/mL at 100 times dilutions. Samples were first tested with 5-minute scans. To minimize background due to photodegradation of the substrate wrapping, single-point measurements were taken for longer tests. Samples were scanned and compared to controls at times of 1 h, 2.5 h, 24 h, and 29 h.

2.4. Benchmarking Sensors with an Established Assay

A colorimetric assay was performed in a multiwell plate using the Pierce Colorimetric Protease Assay Kit (Fisher 23263). A 2.5 mg/mL casein (Carolina 853428) solution was prepared in a pH 8.5 borate buffer. Proteolysis was initiated by adding 25 μL protease solution to 100 μL of the casein solution, and the reaction was incubated for 20 min. 50 μL of 5% w/v 2,4,6-trinitrobenzene sulfonic acid were added to the solution followed by an additional 20 minutes of incubation. Absorbance at 450 nm was measured and compared to controls. This signal difference was then correlated with logarithm of enzyme concentration. A bacterial protease sample was tested compared to a trypsin standard curve with 10-times serial dilutions. Using the fluorescent SWNT probe assay (2.5 mg/mL casein solution) two activity curves were produced using 2-times serial dilutions of both proteases. Protease concentrations were selected based on the results of the Pierce colorimetric assay.

2.5. Detection of Freeze-Thaw Damage

A 5-mL concentrated enzyme sample was repeatedly flash-frozen in liquid nitrogen and thawed in a 37 °C water bath. Before and after each cycle, enzyme activity was measured using the fluorescent assay. This was repeated for 10 freeze-thaw cycles.

2.6. Heat Damage to Cellulase

400 μL samples of cellulase solution were aliquoted into 2-mL Eppendorf tubes and placed into a heating block (Eppendorf Thermomixer C) at selected temperatures. After incubation for a set amount of time, the tube was removed from the heat block and cooled to room temperature. The samples were then tested with the fluorescent assay. This procedure was repeated with bacterial protease and pectinase solutions.

2.7. Determining Optimal Reaction Conditions

The effect of temperature and pH was determined according to a face-centered experimental design. A fixed-temperature container was made using a clear-bottom petri dish (Mattek P35GCOL-0-10-C) with a brass compression sleeve fixed at the center (Supplement 7.1). CMC-SWNT solutions were diluted from 10 mg/mL to 2 mg/mL solutions with phosphate-citric acid buffers. Buffer solutions were preheated in a constant temperature bath, and temperature was maintained by filling the outer portion of the vessel with water from the bath.

3. Results and Discussion

3.1. Hydrolytic Enzyme Sensors

(6,5)-chiral SWNT (diameter = 0.76 nm, excitation = 567 nm, emission = 975 nm) were chosen as the sensor backbone due to their stable near-infrared fluorescence and ease of production by Co-Mo catalysts[30,46]. The hydrophobic SWNT were suspended in water by wrapping them with amphiphilic, macromolecular substrates, materials with molar masses ranging from 15 kDa to 250 kDa that featured both hydrophilic and hydrophobic moieties. SWNT were dispersed by sonication in the presence of target enzyme substrate and recovered as supernatant after centrifugation. While the SWNT sensors were functional with all tested amphiphilic substrates, the sensitivity and repeatability were affected by the substrate's affinity to the nanotube material and resulting fluorescent quality. Thus, SWNT wrapped tightly with carboxymethylcellulose, a stable species that is predominately hydrophobic, would exhibit higher sensitivity and lower response variability than SWNT wrapped loosely with demethoxylated pectin, a species that is mostly hydrophilic. Unlike other complex hydrolytic enzyme activity probes, manufacture of each, new SWNT sensor was straightforward, with complete synthesis in less than one hour. The absence of linking chemistry made this a highly modular assay. Sensor

stability was largely dependent on the stability of the substrate. BSA-, pectin-, and CMC-wrapped SWNT remained stable for approximately 3 months, 1 week, and 1 year respectively. To demonstrate the modularity, sensors were made with a variety of enzyme-substrate pairs to show transduction of protein, oligosaccharide, and polysaccharide hydrolysis.

To interrogate the SWNT sensor, a new low-cost, open source detector was developed. An optical sensor can only find utility if its requisite illumination source and detector are on the size and cost scale of the intended application[47]. In this case, the widespread use of hydrolytic enzymes as agricultural and industrial catalysts as an application does not support the traditional inverted microscope coupled to high cost lasers and detectors. The reader designed for this work was an improved model from previous efforts to create portable SWNT detection[48]. The advances have increased the signal to noise quality and provide a price point below $2500 (Supplement 1). The reader uses a 565 nm LED diode as an excitation source, an InGaAs amplified avalanche photodetector to measure emission (Figure 1a), and a low-cost single board computer (Raspberry Pi 3 – Supplement 2.1) to digitally record the signal.

Hydrolytic activity was measured by adding a small volume of concentrated enzyme solution to the sensor solution and recording decrease to fluorescent signal with respect to time (Figure 1b). After decomposition of the wrapping, SWNT were rendered insoluble in water, causing them to agglomerate (Figure 1c). This agglomeration event was confirmed at the microscale by AFM (Supplement 9). While decrease in fluorescence signal was believed to have been caused by a self-quenching effect (Figure 1d), it may also be influenced by a dielectric shift caused by exposure of the nanotube surface directly to water[40]. Spectral data collected while testing BSA-SWNT with subtilisin showed a decrease of peak height and an absence of any spectral shift, suggesting quenching to be the dominant transduction mechanism (Supplement 12). Tests of fluorescent sensors immobilized on an agarose surface still show the quenching event to be possible if the nanotubes are at high enough concentration to have proximal neighbors (Supplement 8). Lack of signal change with thermally deactivated enzyme confirmed that the sensor response resulted from enzyme activity and not matrix elements in samples, and the responses from other, non-corresponding enzymes confirmed that the selectivity of the sensor matched the selectivity of the substrate (Supplement 11). In other tests, negative controls were used by adding deionized water to samples in place of enzymes to distinguish response *vs.* modulation caused by volumetric change. Values obtained from these controls were subtracted from those obtained with enzyme samples.

Conversion was determined as a function of signal change, which was normalized after completion of reaction according to the following equation:

$$X_S = \frac{I_0 - I}{I_0 - I_E} \quad (1)$$

Where X_S is the observed substrate conversion, I is the instantaneous fluorescent signal intensity, I_o is the starting intensity, I_E is the final, steady-state intensity for each enzyme substrate pair measured when signal stabilized (1-3 h incubation). This normalization inverts the decreasing, quenched signal response (Figure 1b) into a positive response (Figure 2). The normalized data was then smoothed by Fourier deconvolution (Supplement 2.3-2.5). While steady-state fluorescence signal was consistent among individual enzymes, it varied among different enzyme types. For example, fluorescence of casein-wrapped SWNT reached background levels after proteolysis by bacterial protease whereas CMC-wrapped SWNT remained at higher fluorescence values, likely due to cellulase's inability to hydrolyze carboxymethyl- substituted monomers[49]. These differences likely resulted from the enzyme's inability to completely digest a fraction of the suspended SWNT. It was also possible that, while SWNT are rendered insoluble, remnant substrate wrappings could also have prevented direct contact among SWNT, decreasing FRET efficiency and limiting the quenching effect. In each assay the end fluorescence (I_E) was experimentally acquired for use in data normalization. After

normalization, comparisons could be made between experiments and kinetic parameters could be determined.

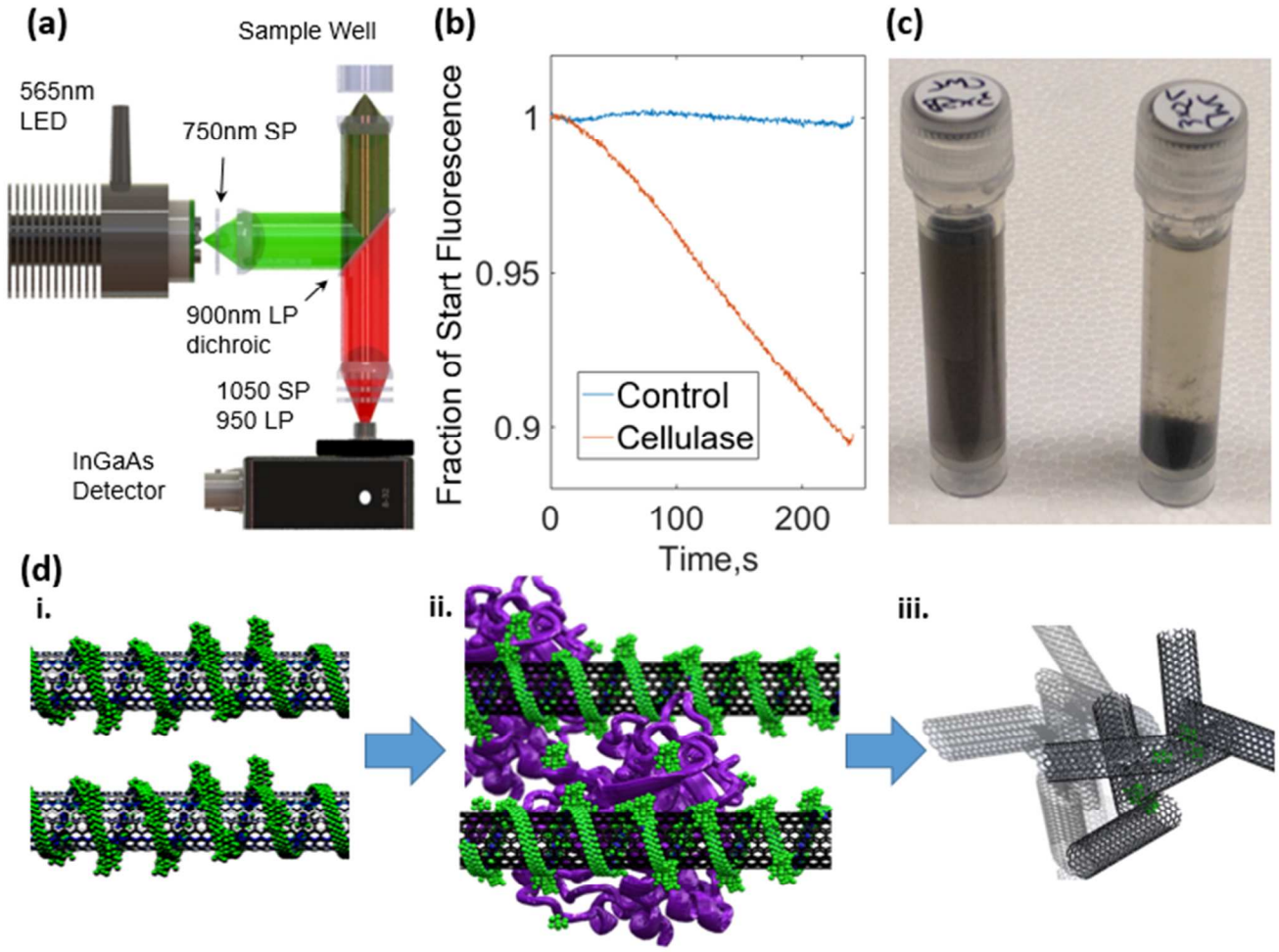

Figure 1. **(a)** Schematic of low cost near-infrared fluorimeter. **(b)** Normalized SWNT sensor fluorescence signal versus time for water addition (control) and cellulase (response). **(c)** Left: Sample of CMC-wrapped nanotubes. Right: 1 hour after addition of cellulase, nanotubes agglomerate and settle at bottom. **(d)** Proposed mechanism of sensing: (i) nanotubes are solubilized by amphiphilic polymer and nanotubes fluoresce, (ii) wrapping is removed due to enzyme hydrolysis, and (iii) nanotubes agglomerate causing quenched signal.

3.2. Determining Kinetic Parameters

To determine kinetic parameters, sensor responses were obtained at a range of enzyme concentrations. The anticipated, positive correlation between rate of signal change and enzyme concentration was observed for bacterial protease to BSA, pectinase to pectin, and cellulase to CMC (Figure 2a-c). The responses appeared to fit with first-order, substrate-limited enzyme kinetics. The relative rates from each experiment were determined based on fitted models (Supplement 2.6) and these were plotted against the enzyme concentration (Figure 2d). Thus, the limiting regime was immediately apparent in the shape of the response.

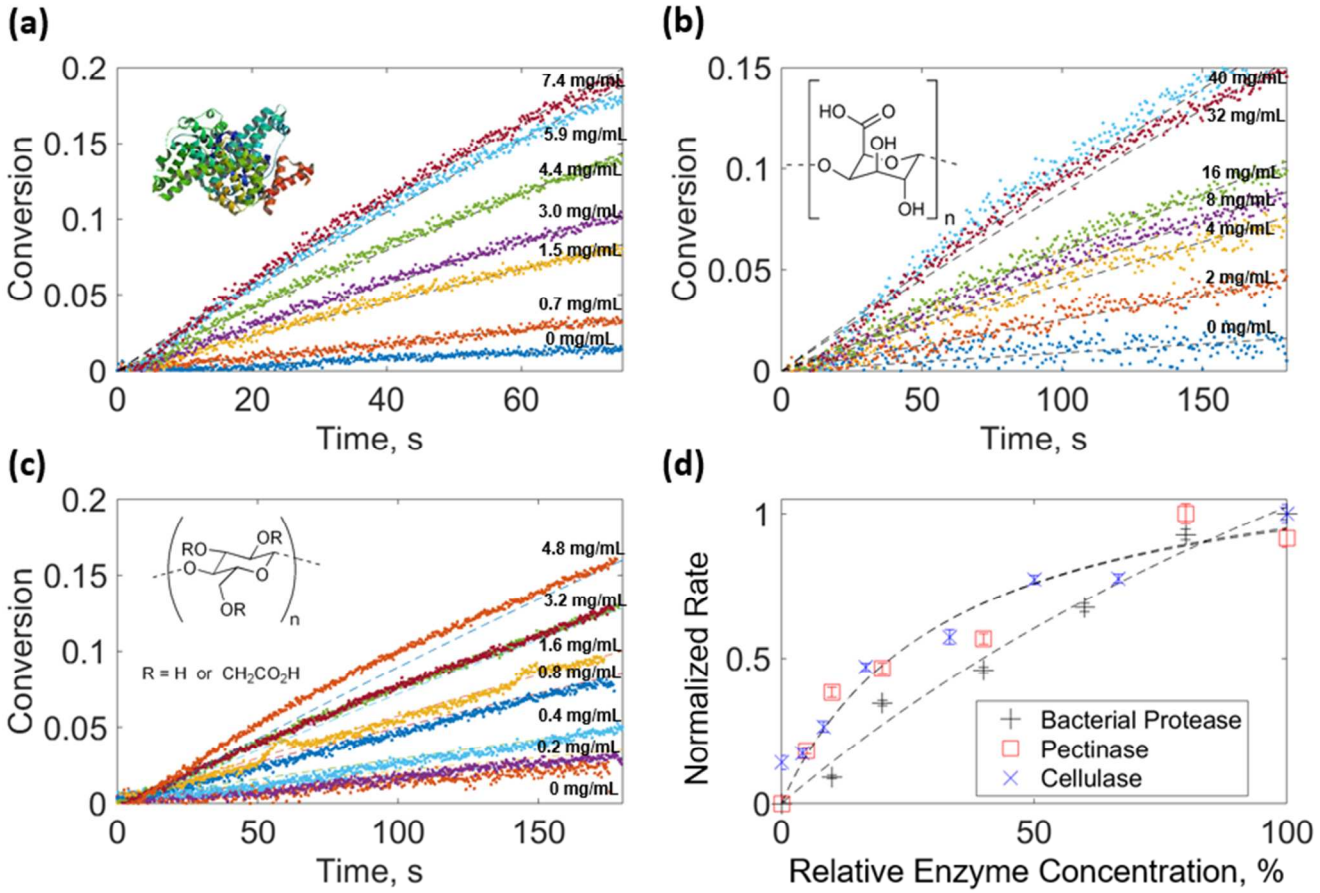

Figure 2. Observed conversion profiles at different enzyme concentrations depict extent of reaction over time for **(a)** BSA and bacterial protease, **(b)** pectin and pectinase, and **(c)** CMC and cellulase. **(d)** Different rate vs enzyme concentration patterns observed for different enzymes

Kinetic parameters, or observed rate constants, were fit to the relative rate *vs.* enzyme concentration data (dotted lines in Figure 2d). For a substrate-limited response, substrate concentration must be redefined as a sum of comparable free and enzyme-bound quantities:

$$[S]_T = [S] + [ES] \quad (2)$$

Where $[S]_T$ is the total substrate concentration, [S] is the unbound substrate concentration, and [ES] is the enzyme-bound substrate concentration. Applying this balance, the rate of substrate consumption may be approximated[50]:

$$\frac{d[S]_T}{dt} = -\frac{k_{cat}[E]_T[S]_T}{K_M+[E]_T+[S]_T} \quad (3)$$

Where t is time, k_{cat} is turnover frequency, $[E]_T$ is the total enzyme concentration, K_M is the Menten constant. Assuming substrate concentration in the denominator to be negligible, observed first order rate constants could be fitted to the below equation:

$$\frac{d[S]_T}{dt} = -\frac{k_{cat}[E]_T[S]_T}{K_M+[E]_T} \quad (4)$$

With tests at multiple enzyme concentrations, catalytic turnover frequencies of $3.785 \pm 2.495 \times 10^{-3}$, $1.080 \pm 0.476 \times 10^{-3}$, and $2.354 \pm 0.391 \times 10^{-3}$ $g_{substrate}/g_{cat}$ s^{-1} were determined for the bacterial subtilisin, pectinase, and cellulase respectively at a pH of 7 and a temperature of approximately 20 ºC. High variability of calculated constants may be associated with inconsistencies in running this assay by hand, such as the pipetting of enzyme solutions and manual positioning of samples over the detection apparatus, which will be mitigated by subsequent automation. Comparison of these terms to published

values is complicated due to the common use of enzyme "activity units," which report activity with respect to a specific substrate (*e.g.* trypsin units for proteases, galacturonidase units for pectinases, and filter paper units for cellulases) and only describe relative enzyme activities[51–54]; this inability to compare enzyme activity units to actual substrate degradation rates demonstrates the need for an assay such as this.

3.3. Establishing Detection Limit

The detection limit was established with Proteinase K, a subtilisin-like protease selected for its stable and well-characterized activity. Within 5 minutes, signal changes were measurable at enzyme concentrations as low as 500 nM. When incubated for 24-29 h, the sensors yielded a statistically significant response with enzyme concentrations as low as 5 fM (Supplement 3). Longer assay times for low concentration enzyme characterization would be acceptable with an automated scanning apparatus where many tests could be conducted in parallel.

3.4. Benchmarking Sensors with an Established Assay

To confirm utility of these hydrolytic enzyme sensors, the fluorescent assay was compared to an established colorimetric assay (Figure 3). The Pierce colorimetric protease assay kit was used to detect hydrolytic activity of a crude bacterial protease sample and a trypsin standard. Proteolytic activity was chosen due to the ease of wrapping SWNT with amphiphilic proteins and the existence of a standardized assay. Both the colorimetric and the fluorescent assays were performed at the same pH, temperature, and substrate concentration. Scans without substrate were used as negative controls to subtract any signal change (*e.g.* background) produced by the enzyme samples.

Direct sensitivity to enzyme activity made the fluorescence assay a more precise alternative. While the logarithmic sensitivity of the colorimetric assay would yield a large dynamic range, this was found to be at the cost of precision, as errors spanned orders of magnitude at enzyme concentrations greater than 100µg/ml. Thus, this colorimetric assay appears to be limited to applications with enzyme working concentrations of 1 to 100µg/ml such as purification and tracking of contamination, while the fluorescent assay could be used for enzyme activity measurements at higher concentrations, such as optimization studies of industrial biocatalysts.

One difficulty in using the colorimetric assay was diluting samples to fit within the dynamic range. Because the colorimetric assay tracked appearance of hydrolysis byproducts rather than disappearance of substrates, responses were susceptible to interference by species already present in sample. As a result, the dynamic range varied on a sample-by-sample basis. For example, of seven crude subtilisin samples, four returned erroneous data. This problem was compounded by a 40-minute response time. The single time-point nature of the colorimetric assay data also limited experiments to linear, enzyme-limited responses. In contrast, the fluorescent assay measured the rate of substrate disappearance and was thus tolerant of more complex samples with contents that would otherwise interfere with the assay. In 3-5 minutes, real-time data could be used to track enzyme activity in either enzyme-limited or substrate-limited regimes.

A second difficulty in using the colorimetric assay was timing of absorbance measurements. At incubation times greater than 20 minutes, color continued to develop, and sample absorbances would become indistinguishable. Because the pipetting process was not instantaneous, data was susceptible to significant error from timing of measurements. The long response time of such colorimetric assays would necessitate parallel tests which would guarantee such error. While this error could be lowered by either using a multichannel pipette or reducing the number of parallel tests, these would require a larger sample volume or a lower throughput respectively.

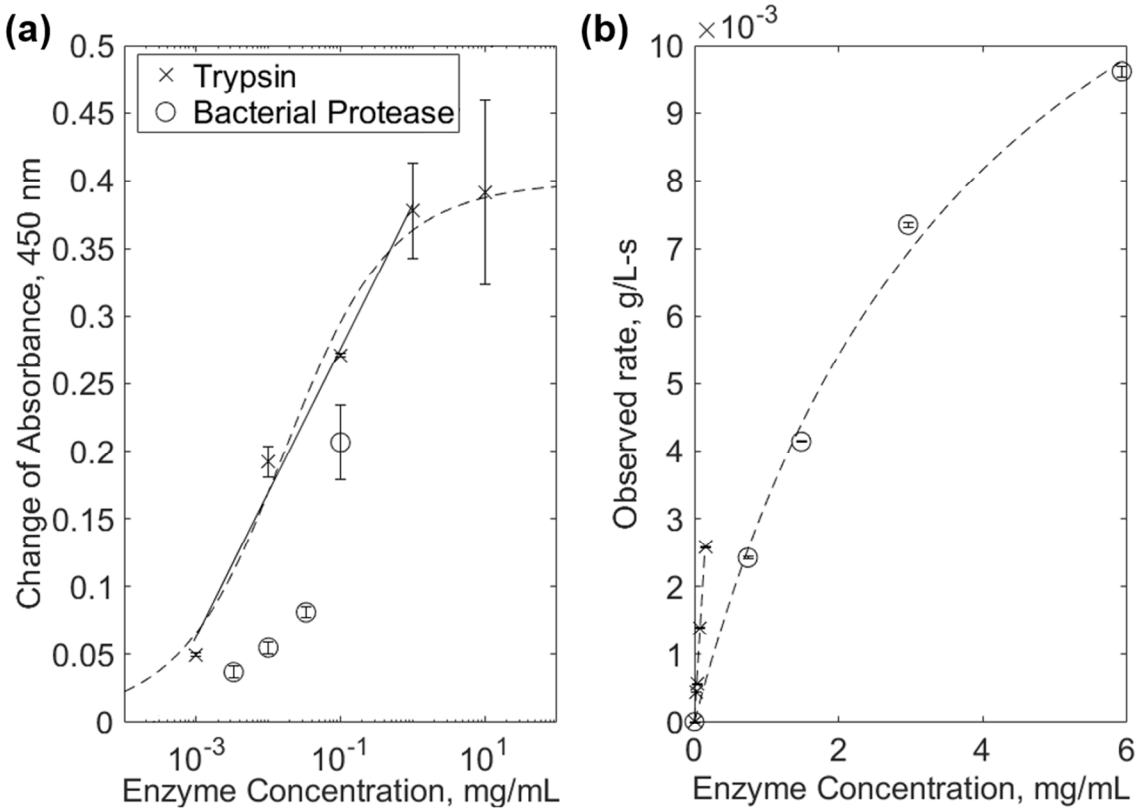

Figure 3. Procedural comparison of fluorescent and colorimetric assays. **(a)** Using the Pierce colorimetric assay, protease activity was fit to a linear curve (solid line) which described the region of sensitivity and a 4-point logistic curve (dashes) which better describes the data at all concentrations sampled on a semi-log plot. Error increased greatly with increased sample concentrations and deviated from linear behavior. Crude subtilisin samples were compared to a trypsin standard curve **(b)** Using the nanotube fluorescent assay, protease activity was compared to the same trypsin standard. Relative error is comparatively small at high enzyme concentrations.

3.5. Monitoring Damage to Enzymes

One potential application of this assay is the monitoring of damage to hydrolytic enzymes. Damage to enzymes can occur during purification, compounding, storage (where samples are frozen and thawed), and during transportation (where samples may be exposed to elevated temperatures). To demonstrate the utility of these sensors for this application, activities of bacterial protease, pectinase, and cellulase were measured after freeze-thaw cycles and exposure to high temperatures. Freeze-thaw damage had previously been shown to be extremely variable, depending on freezing temperature, storage time, enzyme concentrations, and matrix elements, varying from no damage to exponential loss of activity with successive freeze-thaw cycles[55–57]. Response profiles were recorded after repeatedly flash-freezing enzyme samples, and predicted rate constants were compared. While measured activity was observed to fluctuate (especially for the more unstably wrapped pectin-SWNT), no significant trend was observed between the number of freeze-thaw cycles and enzyme activity (Figure 4a). Irreversible heat damage to bacterial protease, pectinase, and cellulase was measured at temperatures of 60, 70, and 95 ˚C (Figure 4b-d). Of the three, cellulase was found to be most sensitive to heat while bacterial protease remained functional until near-boiling conditions. High thermal stability of bacterial protease was expected when considering its widespread industrial use. Activity profiles of pectinase agreed with a prior study that calculated the half-life of this pectinase to be approximately 5 and 3 minutes at 60 and 70 ˚C respectively[58].

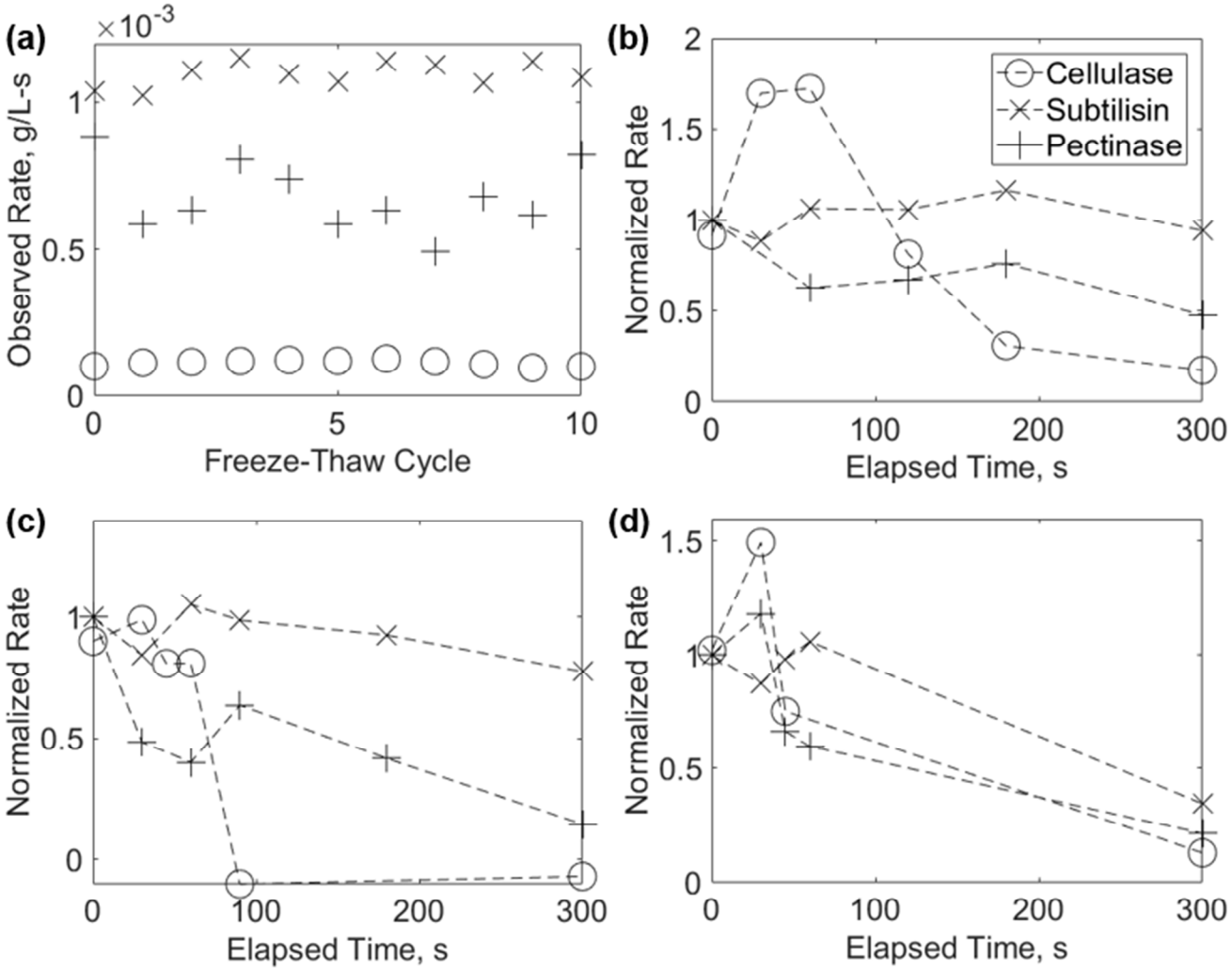

Figure 4. (a) Observed reaction rate versus number of elapsed freeze-thaw cycles indicates minimal damage to enzyme catalysts. **(b)** Thermal degradation tests at 60 ˚C. Only subtilisin appears to be stable. Cellulase is the least stable. **(c)** Thermal degradation tests at 70 ˚C. Both cellulase and pectinase activities approach zero. Subtilisin activity begins to diminish. **(d)** Thermal degradation tests at 95 ˚C. All three enzyme activities approach zero.

3.6. Determining Optimal Reaction Conditions

Lastly, a response surface was constructed to demonstrate this assay's viability as a tool to rapidly determine optimal operating conditions for new industrial enzymes. A face-centered, central composite design was used to produce a quadratic surface response model for the cellulase-CMC system with respect to pH and temperature (Figure 5, model equation and goodness of fit statistics are in Supplement 7.3). A strong dependence was observed with respect to pH while a weaker dependence was observed with respect to temperature, likely due to the small selected temperature range. This assay's response time allowed completion of the statistical optimization campaign within two hours with serial measurements. Improvement to a parallel scanning near-infrared fluorimeter would reduce the necessary time for new enzyme optimization to minutes.

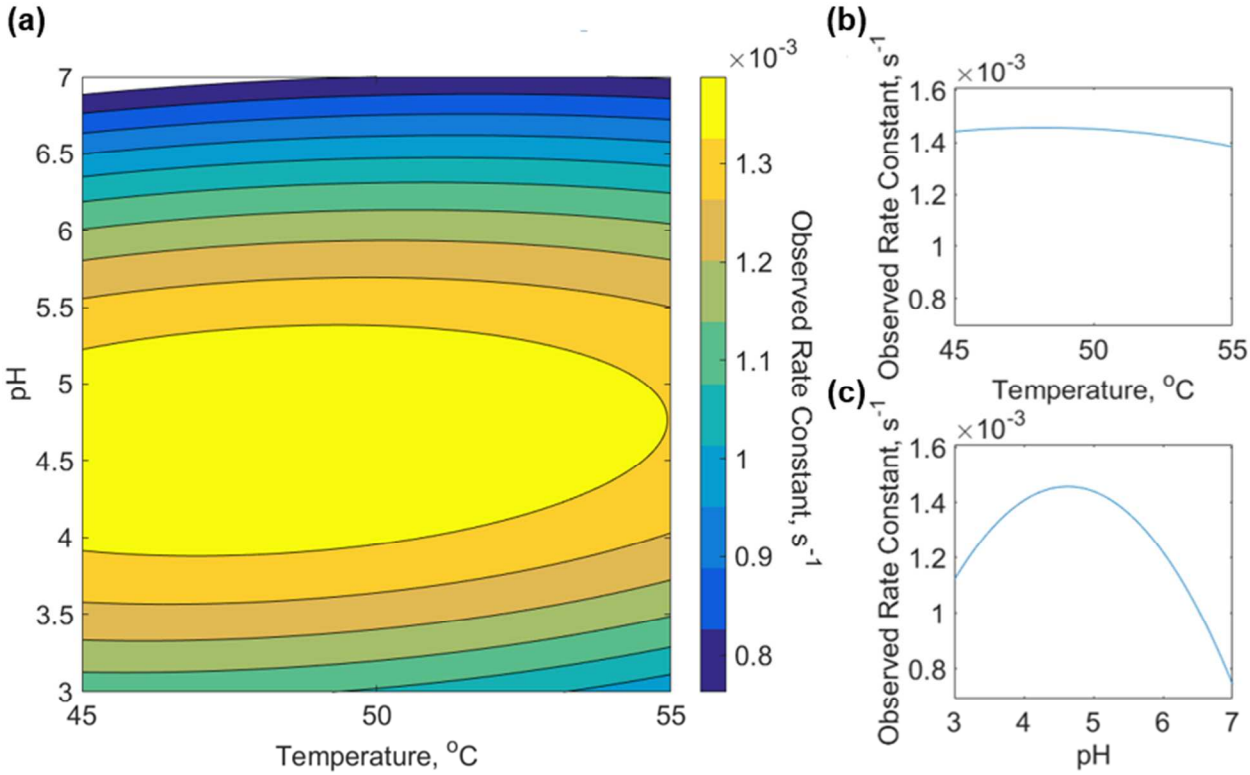

Figure 5. **(a)** Surface response model of observed cellulase activity vs pH and temperature from designed experiments. Optimal conditions occurred at temperature of 48.2 ˚C and pH of 4.63. Model plotted with data points available in Supplement 7. **(b)** Rate vs temperature at optimal pH shows low sensitivity to temperature. **(c)** Rate vs pH at optimal temperature shows high sensitivity to pH.

4. Conclusion

In summary, this sensing platform can be easily and rapidly synthesized to detect the depletion of a hydrolytic enzyme substrate in real time. This sensor has been demonstrated to be versatile by screening three different types of substrate and enzyme combinations. Depletion of substrate can be correlated with signal change to predict quantitative rate constants. Comparison with an established colorimetric assay demonstrates high performance in complex, otherwise-difficult samples. This assay can be used to rapidly track changes in enzyme activity to monitor damage or to perform optimization campaigns.

This sensor's versatility, unique size scale, and penetrating near-infrared spectral window make it suitable for a range of enzyme-related applications. Of interest to industrial biotechnology will be speed and simplicity enhancement to routine optimization studies where new mutant hydrolase enzymes are screened to determine optimal operating conditions. For medical applications, this tool could be used for *in vivo* zymography, or the tracking of temporal and spatial dynamics of health-related enzymes such as MMPs from tumors. For drug development, these sensors could be used in the design and screening of hydrolase inhibitors. Lastly, for food production these tools could be used to test and design cost-effective immobilization strategies for hydrolases in routine processing such as saccharification[6,59]. As these applications are pursued the SWNT reader portability, sensitivity, and cost can also be improved. Sensor manufacturing conditions and wrapping properties may also be screened to optimize sensor stability, sensitivity, and selectivity.

Acknowledgements

This work was supported by Iowa State University startup funds to NFR.

Supporting Information

Supplement.pdf

In this file, the fluorimeter apparatus is described in further detail, methods of data processing are described, and cellulase optimization statistics are provided. AFM characterization of the probes, a selectivity test, and the probe's spectral response are also provided in the supplement.

References

(1) Boyce, S.; Tipton, K. F.; Ako, H.; Nip, W. K. Enzyme Classification and Nomenclature. *eLS* **2001**, 135–154.

(2) Dong, Y.; Zhang, L. Quorum Sensing and Quorum-Quenching Enzymes. **2005**, *43*, 101–109.

(3) Vorwerk, S.; Somerville, S.; Somerville, C. The Role of Plant Cell Wall Polysaccharide Composition in Disease Resistance. *Trends Plant Sci.* **2004**, *9*, 203–209.

(4) King, B. C.; Waxman, K. D.; Nenni, N. V.; Walker, L. P.; Bergstrom, G. C.; Gibson, D. M. Arsenal of Plant Cell Wall Degrading Enzymes Reflects Host Preference among Plant Pathogenic Fungi. *Biotechnol Biofuels* **2011**, *4*, 1-14.

(5) Deryugina, E. I.; Quigley, J. P. Matrix Metalloproteinases and Tumor Metastasis. *Cancer Metastasis Rev.* **2006**, *25*, 9–34.

(6) Fernandes, P. Enzymes in Food Processing: A Condensed Overview on Strategies for Better Biocatalysts. *Enzyme Res.* **2010**, *2010*, 1–19.

(7) Singh, R.; Kumar, M.; Mittal, A.; Mehta, P. K. Microbial Enzymes: Industrial Progress in 21st Century. *3 Biotech* **2016**, *6*, 1–15.

(8) Li, S.; Yang, X.; Yang, S.; Zhu, M.; Wang, X. Technology Prospecting on Enzymes: Application, Marketing and Engineering. *Comput. Struct. Biotechnol. J.* **2012**, *2*, 1-11.

(9) Wichmann, O.; Wittbrodt, J.; Schultz, C. A Small-Molecule FRET Probe to Monitor Phospholipase A2 Activity in Cells and Organisms. *Angew. Chemie.* **2006**, *45*, 508–512.

(10) Resch-Genger, U.; Grabolle, M.; Cavaliere-Jaricot, S.; Nitschke, R.; Nann, T. Quantum Dots versus Organic Dyes as Fluorescent Labels. *Nat. Methods* **2008**, *5*, 763–775.

(11) Chang, E.; Miller, J. S.; Sun, J.; Yu, W. W.; Colvin, V. L.; Drezek, R.; West, J. L. Protease-Activated Quantum Dot Probes. *Biochem. Biophys. Res. Commun.* **2005**, *334*, 1317–1321.

(12) Kim, G. B.; Kim, Y.-P. Analysis of Protease Activity Using Quantum Dots and Resonance Energy Transfer. *Theranostics* **2012**, *2*, 127–138.

(13) Michalet, X.; Pinaud, F. F.; Bentolila, L. A.; Tsay, J. M.; Doose, S.; Li, J. J.; Sundaresan, G.; Wu, A. M.; Gambhir, S. S.; Weiss, S. Quantum Dots for Live Cells, in Vivo Imaging, and Diagnostics. *Science.* **2005**, *307*, 538–545.

(14) Gill, R.; Willner, I.; Shweky, I.; Banin, U. Fluorescence Resonance Energy Transfer in CdSe / ZnS - DNA Conjugates : Probing Hybridization and DNA Cleavage. *J. Phys. Chem.* **2005**, *109*, 23715–23719.

(15) Kim, Y.-P.; Daniel, W. L.; Xia, Z.; Xie, H.; Mirkin, C. A.; Rao, J. Bioluminescent Nanosensors for Protease Detection Based upon Gold Nanoparticle–luciferase Conjugates. *Chem. Commun.* **2010**, *46*, 76–78.

(16) Yao, H.; Zhang, Y.; Xiao, F.; Xia, Z.; Rao, J. Quantum Dot/bioluminescence Resonance Energy Transfer Based Highly Sensitive Detection of Proteases. *Angew. Chemie Int. Ed.* **2007**, *46*, 4346–4349.

(17) Li, X.; Gao, X.; Shi, W.; Ma, H. Design Strategies for Water-Soluble Small Molecular Chromogenic and Fluorogenic Probes. *Chem. Rev.* **2013**, *114*, 590–659.

(18) Manafi, M. Fluorogenic and Chromogenic Enzyme Substrates in Culture Media and Identification Tests. *Int. J. Food Microbiol.* **1996**, *31*, 45–58.

(19) Almin, K. E.; Eriksson, K.-E. Enzymic Degradation of Polymers. *Biochim. Biophys. Acta* -

Enzymol. **1967**, *139*, 238–247.
(20) Smidsrød, O.; Haug, A.; Lársen, B. Oxidative-Reductive Depolymerization: A Note on the Comparison of Degradation Rates of Different Polymers by Viscosity Measurements. *Carbohydr. Res.* **1967**, *5*, 482–485.
(21) Uribe, S.; Sampedro, J. G. Measuring Solution Viscosity and Its Effect on Enzyme Activity. *Biol. Proced. Online* **2003**, *5*, 108–115.
(22) Rapport, M. M.; Meyer, K.; Linker, A. Correlation of Reductimetric and Turbidimetric Methods for Hyaluronidase Assay. *J. Biol. Chem.* **1950**, *186*, 615–623.
(23) Tietz, N. W.; Shuey, D. F.; Astles, J. R. Turbidimetric Measurement of Lipase Activity--Problems and Some Solutions. *Clin. Chem.* **1987**, *33*, 1624–1629.
(24) Nummi, M.; Fox, P. C.; Niku-Paavola, M.-L.; Enari, T.-M. Nephelometric and Turbidometric Assays of Cellulase Activity. *Anal. Biochem.* **1981**, *116*, 133–136.
(25) Sapan, C. V; Lundblad, R. L.; Price, N. C. Colorimetric Protein Assay Techniques. *Biotechnol. Appl. Biochem.* **1999**, *29*, 99–108.
(26) Gusakov, A. V.; Kondratyeva, E. G.; Sinitsyn, A. P. Comparison of Two Methods for Assaying Reducing Sugars in the Determination of Carbohydrase Activities. *Int. J. Anal. Chem.* **2011**, *2011*, 1–4.
(27) Rivers, D. B.; Gracheck, S. J.; Woodford, L. C.; Emert, G. H. Limitations of the DNS Assay for Reducing Sugars from Saccharified Lignocellulosics. *Biotechnol. Bioeng.* **1984**, *26*, 800–802.
(28) Olson, B. J. S. C.; Markwell, J. Assays for Determination of Protein Concentration. *Curr. Protoc. protein Sci.* **2007**, 3.4.1–3.4.29.
(29) Smith, A. M.; Mancini, M. C.; Nie, S. Bioimaging: Second Window for in Vivo Imaging. *Nat. Nanotechnol.* **2009**, *4*, 710–711.
(30) Bachilo, S. M.; Strano, M. S.; Kittrell, C.; Hauge, R. H.; Smalley, R. E.; Weisman, R. B. Structure-Assigned Optical Spectra of Single-Walled Carbon Nanotubes. *Science.* **2002**, *298*, 2361–2366.
(31) Kruss, S.; Hilmer, A. J.; Zhang, J.; Reuel, N. F.; Mu, B.; Strano, M. S. Carbon Nanotubes as Optical Biomedical Sensors. *Adv. Drug Deliv. Rev.* **2013**, *65*, 1933–1950.
(32) Heller, D. A.; Pratt, G. W.; Zhang, J. Q.; Nair, N.; Hansborough, A. J.; Boghossian, A. A.; Reuel, N. F.; Barone, P. W.; Strano, M. S. Peptide Secondary Structure Modulates Single-Walled Carbon Nanotube Fluorescence as a Chaperone Sensor for Nitroaromatics. *Proc. Natl. Acad. Sci. U. S. A.* **2011**, *108*, 8544–8549.
(33) Kim, J.-H.; Patra, C. R.; Arkalgud, J. R.; Boghossian, A. a; Zhang, J.; Han, J. H.; Reuel, N. F.; Ahn, J.-H.; Mukhopadhyay, D.; Strano, M. S. Single-Molecule Detection of H_2O_2 Mediating Angiogenic Redox Signaling on Fluorescent Single-Walled Carbon Nanotube Array. *ACS Nano* **2011**, *5*, 7848–7857.
(34) Zhang, J.; Landry, M. P.; Barone, P. W.; Kim, J. H.; Lin, S.; Ulissi, Z. W.; Lin, D.; Mu, B.; Boghossian, A. A.; Hilmer, A. J.; Rwei, A.; Hinckley, A. C.; Kruss, S.; Shandell, M. A.; Nair, N.; Blake, S.; Sen, F.; Sen, S.; Croy, R. G.; Li, D.; Yum, K.; Ahn, J.; Jin, H.; Heller, D. A.; Essigmann, J. M.; Blankschtein, D.; Strano, M.S. Molecular Recognition Using Corona Phase Complexes Made of Synthetic Polymers Adsorbed on Carbon Nanotubes. *Nat. Nanotechnol.* **2013**, *8*, 959–968.
(35) Mu, B.; McNicholas, T. P.; Zhang, J.; Hilmer, A. J.; Jin, Z.; Reuel, N. F.; Kim, J.-H.; Yum, K.; Strano, M. S. A Structure-Function Relationship for the Optical Modulation of Phenyl Boronic Acid-Grafted, Polyethylene Glycol Wrapped Single Walled Carbon Nanotubes. *J. Am. Chem. Soc.* **2012**, 1–18.
(36) Reuel, N. F.; Ahn, J.; Kim, J.-H.; Zhang, J.; Boghossian, A. a; Mahal, L. K.; Strano, M. S. Transduction of Glycan–lectin Binding Using near-Infrared Fluorescent Single-Walled Carbon

Nanotubes for Glycan Profiling. *J. Am. Chem. Soc.* **2011**, *133*, 17923–17933.
(37) Zhang, J.; Boghossian, A. A.; Barone, P. W.; Rwei, A.; Kim, J. H.; Lin, D.; Heller, D. A.; Hilmer, A. J.; Nair, N.; Reuel, N. F.; Strano, M. S. Single Molecule Detection of Nitric Oxide Enabled by d(AT) $_{15}$ DNA Adsorbed to Near Infrared Fluorescent Single-Walled Carbon Nanotubes. *J. Am. Chem. Soc.* **2011**, *133*, 567–581.
(38) Heller, D. A.; Jeng, E. S.; Yeung, T. K.; Martinez, B. M.; Moll, A. E.; Gastala, J. B.; Strano, M. S. Optical Detection of DNA Conformational Polymorphism on Single-Walled Carbon Nanotubes. *Science.* **2006**, *311*, 508–511.
(39) Ahn, J. H.; Kim, J. H.; Reuel, N. F.; Barone, P. W.; Boghossian, A. A.; Zhang, J.; Yoon, H.; Chang, A. C.; Hilmer, A. J.; Strano, M. S. Label-Free, Single Protein Detection on a near-Infrared Fluorescent Single-Walled Carbon Nanotube/protein Microarray Fabricated by Cell-Free Synthesis. *Nano Lett.* **2011**, *11*, 2743–2752.
(40) Reuel, N. F.; Grassbaugh, B.; Kruss, S.; Mundy; Z., J.; Opel, C.; Ogunniyi, A. O.; Egodage, K.; Wahl, R.; Helk, B.; Zhang, J.; Kalcioglu, Z. I.; Tvrdy, K.; Bellisario, D. O.; Mu, B.; Blake, S. S.; Van Vliet, K. J.; Love, J. C.; Wittrup, K. D.; Strano, M. S. Emergent Properties of Nanosensor Arrays: Applications for Monitoring IgG Affinity Distributions, Weakly Affined Hypermannosylation, and Colony Selection for Biomanufacturing. *ACS Nano* **2013**, *7*, 7472–7482.
(41) Reuel, N. F.; Dupont, A.; Thouvenin, O.; Lamb, D. C.; Strano, M. S. Three-Dimensional Tracking of Carbon Nanotubes within Living Cells. *ACS Nano* **2012**, *6*, 5420–5428.
(42) Iverson, N. M.; Barone, P. W.; Shandell, M.; Trudel, L. J.; Sen, S.; Sen, F.; Ivanov, V.; Atolia, E.; Farias, E.; McNicholas, T. P.; Reuel, N.; Parry, N. M. A.; Wogan, G. N.; Strano, M. S. In Vivo Biosensing via Tissue-Localizable near-Infrared-Fluorescent Single-Walled Carbon Nanotubes. *Nat. Nanotechnol.* **2013**, *8*, 873–880.
(43) Boghossian, A. A.; Zhang, J.; Floch-Yin, F. T. Le; Ulissi, Z. W.; Bojo, P.; Han, J.-H.; Kim, J.-H.; Arkalgud, J. R.; Reuel, N. F.; Braatz, R. D.; Strano, M. S. The Chemical Dynamics of Nanosensors Capable of Single-Molecule Detection. *J. Chem. Phys.* **2011**, *135*, 84124.
(44) Landry, M. P.; Kruss, S.; Nelson, J. T.; Bisker, G.; Iverson, N. M.; Reuel, N. F.; Strano, M. S. Experimental Tools to Study Molecular Recognition within the Nanoparticle Corona. *Sensors (Switzerland)* **2014**, *14*, 16196–16211.
(45) Kruss, S.; Landry, M. P.; Vander Ende, E.; Lima, B. M. A.; Reuel, N. F.; Zhang, J.; Nelson, J.; Mu, B.; Hilmer, A.; Strano, M. Neurotransmitter Detection Using Corona Phase Molecular Recognition on Fluorescent Single-Walled Carbon Nanotube Sensors. *J. Am. Chem. Soc.* **2014**, *136*, 713–724.
(46) Kitiyanan, B.; Alvarez, W. E.; Harwell, J. H.; Resasco, D. E. Controlled Production of Single-Wall Carbon Nanotubes by Catalytic Decomposition of CO on Bimetallic Co–Mo Catalysts. *Chem. Phys. Lett.* **2000**, *317*, 497–503.
(47) Fan, X.; White, I. M.; Shopova, S. I.; Zhu, H.; Suter, J. D.; Sun, Y. Sensitive Optical Biosensors for Unlabeled Targets: A Review. *Anal. Chim. Acta* **2008**, *620*, 8–26.
(48) Nelson, J. T.; Kim, S.; Reuel, N. F.; Salem, D. P.; Bisker, G.; Landry, M. P.; Kruss, S.; Barone, P. W.; Kwak, S.; Strano, M. S. Mechanism of Immobilized Protein A Binding to Immunoglobulin G on Nanosensor Array Surfaces. *Anal. Chem.* **2015**, *87*, 8186–8193.
(49) Reese, E. T.; Siu, R. G. H.; Levinson, H. S. The Biological Degradation of Soluble Cellulose Derivatives and Its Relationship to the Mechanism of Cellulose Hydrolysis. *J. Bacteriol.* **1950**, *59*, 485–497.
(50) Tzafriri, A. R. Michaelis-Menten Kinetics at High Enzyme Concentrations. *Bull. Math. Biol.* **2003**, *65*, 1111–1129.
(51) Rick, W. Trypsin. In *Methods of Enzymatic Analysis (Second Edition), Volume 2*; Elsevier,

1974; pp 1013–1024.
(52) Aramrueang, N.; Zicari, S. M.; Zhang, R. Response Surface Optimization of Enzymatic Hydrolysis of Sugar Beet Leaves into Fermentable Sugars for Bioethanol Production. *Adv. Biosci. Biotechnol.* **2017**, *8*, 51–67.
(53) Mussell, H. W.; Morre, D. J. A Quantitative Bioassay Specific for Polygalacturonases. *Anal. Biochem.* **1969**, *28*, 353–360.
(54) Griffin, H. L. Filter Paper assay—Effect of Time and Substrate Concentration on Cellulase Activity. *Anal. Biochem.* **1973**, *56*, 621–625.
(55) Pearce, R. E.; McIntyre, C. J.; Madan, A.; Sanzgiri, U.; Draper, A. J.; Bullock, P. L.; Cook, D. C.; Burton, L. a; Latham, J.; Nevins, C.; Parkinson, A. Effects of Freezing, Thawing, and Storing Human Liver Microsomes on Cytochrome P450 Activity. *Arch Biochem Biophys* **1996**, *331*, 145–169.
(56) Huen, K.; Richter, R.; Furlong, C.; Eskenazi, B.; Holland, N. Validation of PON1 Enzyme Activity Assays for Longitudinal Studies. *Clin. Chim. Acta* **2009**, *402*, 67–74.
(57) Cheftel, J. C.; Lévy, J.; Dumay, E. Pressure-Assisted Freezing and Thawing: Principles and Potential Applications. *Food Rev. Int.* **2000**, *16*, 453–483.
(58) Ortega, N.; De Diego, S.; Rodríguez-Nogales, J. M.; Perez-Mateos, M.; Busto, M. D. Kinetic Behaviour and Thermal Inactivation of Pectinlyase Used in Food Processing. *Int. J. Food Sci. Technol.* **2004**, *39*, 631–639.
(59) DiCosimo, R.; McAuliffe, J.; Poulose, A. J.; Bohlmann, G. Industrial Use of Immobilized Enzymes. *Chem. Soc. Rev.* **2013**, *42*, 6437.

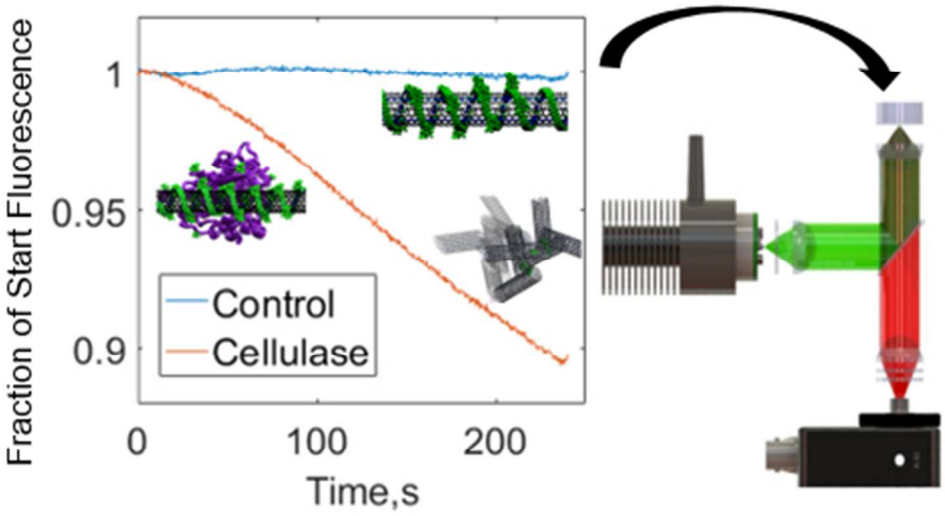

for TOC only

132x74mm (96 x 96 DPI)